Review TRENDS in Neurosciences Vol.28 No.7 July 2005

Synaptic Connectivity series

Neurogeometry and potential synaptic connectivity

Armen Stepanyants[1] and Dmitri B. Chklovskii[2]

[1]Department of Physics and Center for Interdisciplinary Research on Complex Systems, Northeastern University, 110 Forsyth Street, Boston, MA 02115, USA
[2]Cold Spring Harbor Laboratory, 1 Bungtown Road, Cold Spring Harbor, NY 11724, USA

The advent of high-quality 3D reconstructions of neuronal arbors has revived the hope of inferring synaptic connectivity from the geometric shapes of axons and dendrites, or 'neurogeometry'. A quantitative description of connectivity must be built on a sound theoretical framework. Here, we review recent developments in neurogeometry that can provide such a framework. We base the geometric description of connectivity on the concept of a 'potential synapse' – the close apposition between axons and dendrites necessary to form an actual synapse. In addition to describing potential synaptic connectivity in neuronal circuits, neurogeometry provides insight into basic features of functional connectivity, such as specificity and plasticity.

Introduction

Comprehensive understanding of the brain seems impossible without unraveling synaptic connectivity in neuronal circuits. One way of analyzing synaptic connectivity is based on the observation that a synapse requires a physical contact between an axon and a dendrite. Then, spatial overlap of the axonal arbor of a presynaptic neuron with the dendritic arbor of a postsynaptic neuron indicates the possibility of synaptic contacts. Indeed, the utility of neuronal arbor morphology for inferring connectivity has long been recognized [1–11]. However, quantitative and complete geometric description of connectivity has been hindered by the unpredictable nature of the Golgi staining method used to reconstruct arbor shapes (one could never know which neurons were stained and how fully) and by the lack of an adequate computer infrastructure to collect and analyze the data.

With recent technological developments, a comprehensive quantitative geometric description of synaptic connectivity has become an attainable goal. Cell-labeling methods, such as those based on biocytin and green fluorescent protein (GFP), are not only reliable but also enable targeting of specific cell types, defined electrophysiologically or genetically. Labeled cells can be imaged at high resolution using traditional, confocal or two-photon microscopes. Finally, computer-based systems such as Neurolucida (MicroBrightField Inc., http://www.microbrightfield.com/) yield 3D reconstructions of cell shapes in digital vector-based format. Provided data quality and reproducibility are ensured [12,13], such reconstructions can be used for further analysis.

Here, we review a theoretical framework, which we call neurogeometry, developed recently for geometric description of synaptic connectivity. Although geometric description of connectivity can be applied to various neuronal circuits (e.g. those in flies [14] and crickets [15]), in this review we focus on the mammalian neocortex. Interestingly, the significance of neurogeometry goes far beyond inferring connectivity from arbor shapes. The newly developed methods enable one to address important and timely questions about specificity and plasticity in synaptic connectivity.

Potential synapse – a useful concept for geometric description of synaptic connectivity

In describing synaptic connectivity geometrically, it is convenient to use the concept of potential synapse [16]. Potential synapse is a location in the neuropil where an axon is present within distance s of a dendrite so that a synaptic connection can be made (Figure 1). Distance s depends on the type of synapses made by given axons and dendrites. For synapses on spines, s is the typical spine length (i.e. $\sim$2 μm [17–19]). For shaft synapses and gap junctions, s is the sum of dendritic and/or axonal radii (i.e. $\sim$0.4–1.0 μm [6,20]). If a synapse can be made on a terminal bouton, its length determines s. In all three cases, potential synapse is a necessary, but not a sufficient, condition for an actual synapse.

The number of potential synapses between a pair of neurons can be determined directly by jointly reconstructing their axonal and dendritic arbors in 3D and identifying close appositions. Although relevant values of s do not preclude such counts with light microscopy, reconstructing pairs of neurons jointly is difficult and rarely done. To realize fully the power of geometric description, the number of potential synapses must be determined from single-neuron reconstructions, often obtained from different animals. Such single-neuron sampling of potential connectivity has combinatorial leverage because the number of neuronal pairs scales as the number of sampled neurons squared.

Corresponding authors: Stepanyants, A. (a.stepanyants@neu.edu), Chklovskii, D.B. (mitya@cshl.edu).

Available online 2 June 2005

 0166-2236/$ - see front matter doi:10.1016/j.tins.2005.05.006

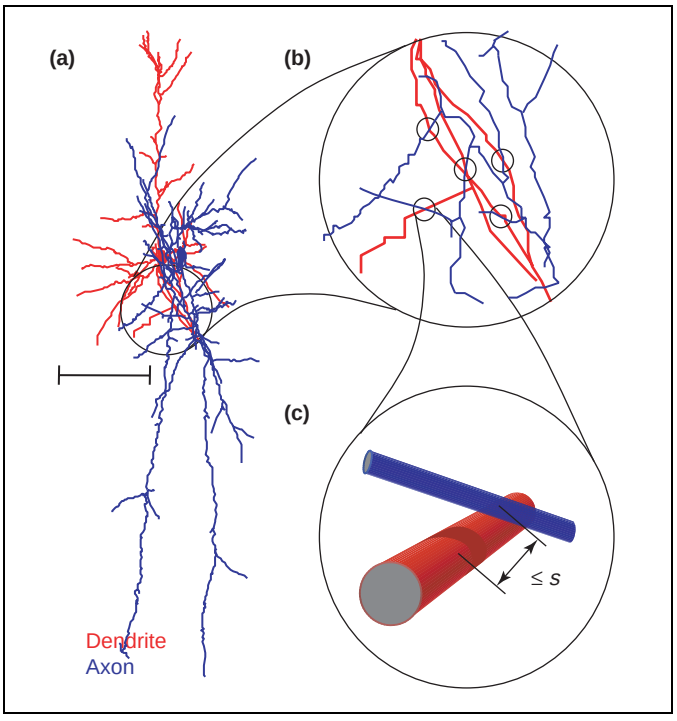

Figure 1. Potential synapses between axonal and dendritic arbors of neighboring neurons. **(a)** A 3D reconstruction of a pyramidal cell dendrite (red) and a regular-spiking non-pyramidal cell axon (blue). **(b)** Magnification of the arbor overlap region. Potential synapses between the two arbors are shown with small black circles. Typically, a pair of neurons with a significant arbor overlap establishes several potential synapses. **(c)** Further magnification of a potential synapse in (b). A potential synapse is a location in the neuropil where an axonal branch is present within certain distance, *s*, of a dendrite. Scale bar: 100 μm in (a), 30 μm in (b), and 3 μm in (c). Modified, with permission, from [43].

Pooling single-neuron reconstructions from different animals adds two complications. First, to combine neurons from different brains correctly one must take into account their position with respect to corresponding anatomical landmarks, such as brain areas, cortical layers or barrels. Because brains differ from animal to animal, registration of landmarks requires morphing the brains to a common template. Second, if after such morphing, branches of corresponding neurons (neurons of the same class and position in the template) differ in location by more than *s* (as inevitably happens in the neocortex), resulting potential connectivity description is only statistical, or probabilistic. However, in the neocortex, this does not diminish the power of the geometric analysis because the relationship of potential and actual synaptic connectivity is statistical by nature (see final section). For certain highly reproducible circuits, such as those in invertebrates (e.g. *Caenorhabditis elegans* [21,22]), statistical description seems less useful than in the cortex.

Because the number of potential synapses depends on neuron identity, informative prediction-making relies on appropriate classification and/or parameterization of neuronal populations. Neurons can be classified on the basis of their morphology, immunohistochemistry, physiology and gene-expression profiles. The resulting classes can also be parameterized based on location in the brain template. In theory, the estimate of geometric connectivity becomes more precise as the neuronal population is divided into finer and finer gradations. In practice, however, the limited size of a sampling dataset defines the reasonable level of gradation.

Evaluation of potential synaptic connectivity can be demonstrated using the cat visual cortex as an example [23,24]. When neurons have been labeled *in vivo* and tissue has been serially sectioned, dendritic and local axonal arbors can be reconstructed in their entirety [25,26]. Neurons can then be classified into pyramidal, spiny stellate and GABAergic types, and parameterized by their laminar location. Figure 2(a) shows a geometric output (or potential divergence) map from a layer 4 spiny stellate neuron (white triangle). The color of each pixel reflects the expected number of potential synapse received by a spiny neuron in that pixel (for details of calculations, see Box 1). Figure 2(b) shows a geometric output map for a layer 2/3 pyramidal cell. Analogous maps can be obtained for geometric input (potential convergence), and output for different classes of neurons with different laminar

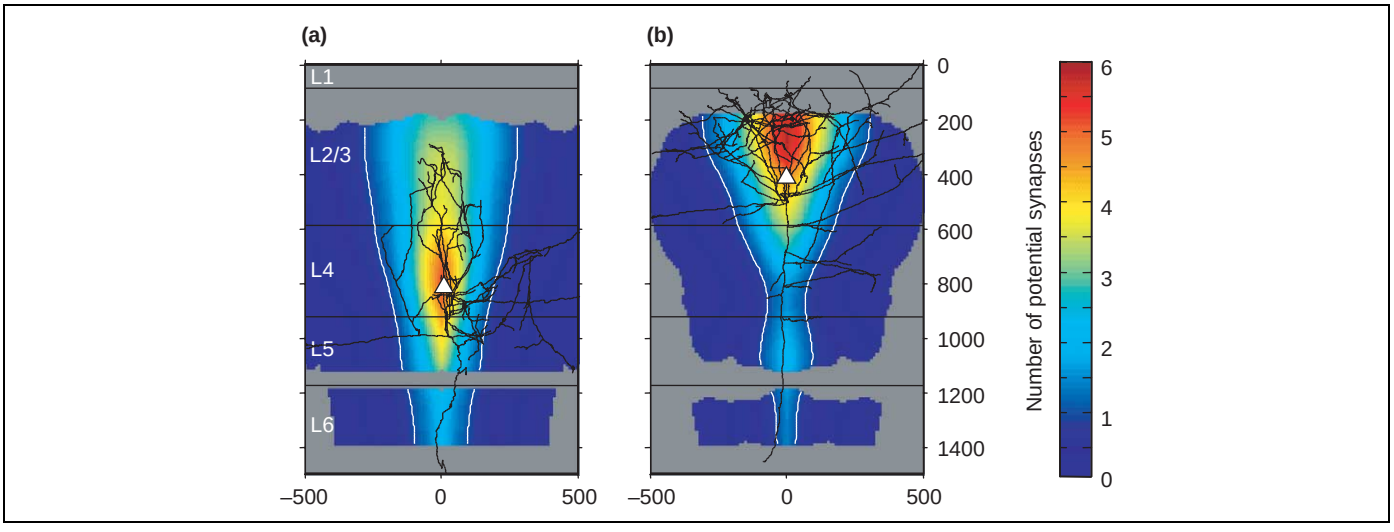

Figure 2. Geometric output maps. **(a)** Expected number of potential synapses made by a lower-layer-4 spiny stellate neuron (soma position is shown with a white triangle) onto other spiny stellate or pyramidal neurons. The color of each pixel indicates the expected number of potential synapses received by a spiny neuron at that location. An example spiny stellate axon with a similar position in the template is shown in black. **(b)** Output map for a layer 3 pyramidal neuron. White contours demarcate the domains of potential divergence of the neurons, where the expected number of potential synapses is greater than one. Gray pixels indicate positions where confidence in the estimate was low owing to a small number of reconstructed arbors. The bottom and right axes show the dimensions of the cortical template (in microns).

Box 1. How to estimate the expected number of potential synapses by using single-neuron reconstructions from different animals

To estimate the number of potential synapses as a function of the relative position of two neurons, one could directly count potential synapses for each arbor pair morphed onto a common template, and then average the results. However, the number of reconstructed neurons is usually small, leading to large fluctuations in potential synapse counts. One way to avoid fluctuation is to average the number of potential synapses over slight variations in the positions of neurons [61]. However, there is also an indirect, but computationally more efficient, way of averaging out the fluctuations.

Reconstructions of neuronal arbors (e.g. Neurolucida files) represent a set of short (1–5 μm) connected straight segments. This set of segments is described by the arbor line (skeleton) density defined as follows (Figure I of this box):

$$\rho^0(\vec{R};\vec{r},\hat{n}) = \sum_i l_i \delta(\vec{r}-\vec{r}_i)\delta(\hat{n}-\hat{n}_i), \qquad \text{(Equation 1)}$$

where ρ^0 (in μm^{-2}) represents the length of neurites with orientation given by unit vector $\hat{n}$ that belong to a unit volume located at $\vec{r}$. Here, $\vec{R}=[x,y,z]$ is the soma position of the reconstructed neuron in the template, δ is the Dirac delta function, and the sum is taken over all segments.

To take into account the expected variability in individual arbor shapes of corresponding neurons and imprecision in measurements, the skeleton density can be convolved with the Gaussian filter G, to yield the density profile:

$$\rho(\vec{R};\vec{r},\hat{n}) = \int \rho^0(\vec{R};\vec{r}',\hat{n})G(\vec{r}-\vec{r}')d^3r' \qquad \text{(Equation 2)}$$

$$G(\vec{r}) = \exp[-\vec{r}^2/2\sigma^2]/(2\pi\sigma^2)^{3/2}$$

For cortical neurons, we adopt the standard deviation, $\sigma \sim 10$–30 μm, which is the typical mesh size of local axonal and dendritic arbors. The number of potential synapses does not depend strongly on particular choice of (in this range. If several reconstructions of corresponding neurons are available, their density profiles can be averaged. If dendritic and local axonal arbors are symmetric around the z-axis perpendicular to the cortical layers [62,63], the density profile can also be made symmetrical by rotation around z [7].

Finally, axonal and dendritic density profiles are combined to estimate the number of potential synapses as a function of neuron positions in the template, $\vec{R}_a$ and $\vec{R}_d$ (for detailed derivation see [64]):

$$N_p(\vec{R}_a,\vec{R}_d) = 2s\int \rho_a(\vec{R}_a;\vec{r}_a,\hat{n}_a)\rho_d(\vec{R}_d;\vec{r}_d,\hat{n}_d)$$

$$\times|\sin(\hat{n}_a,\hat{n}_d)|\delta(\vec{r}_a-\vec{r}_d)d^3r_a d^3r_d d\Omega_a d\Omega_d \qquad \text{(Equation 3)}$$

where s is the distance entering the definition of the potential synapse, $|\sin(\hat{n}_a,\hat{n}_d)|$ is the absolute value of sin of the angle between unit vectors $\hat{n}_a$ and $\hat{n}_d$, and $d\Omega_{a,d}$ denotes integration over all orientations of the unit vectors, $\hat{n}_{a,d}$. Note that the number of potential synapses scales linearly with distance s.

Previously, a simplified version of this expression was derived under assumption of isotropic axonal or dendritic arbors [65,66]. The simplified expression was used to estimate the number of proximities between axons and dendrites [5,66], assuming that length densities follow certain algebraic functions, such as exponentials. Liley and Wright [64] derived the complete expression, taking into account the angular dependence of the line density. Later, several estimates of expected numbers of potential synapses have been made using experimentally measured length densities [7,8,23,24]. All of these methods rely on the assumption that the spatial locations of dendritic and axonal branches are uncorrelated (see main text).

In practice, numerical integration in Equation 3 is computationally expensive and can be avoided by using the following expression, obtained by substituting Equations 1 and 2 into Equation 3:

$$N_p(\vec{R}_a,\vec{R}_d) = 2s\sum_{i,j} l_a^i l_d^j \left|\sin\left(\hat{n}_a^i,\hat{n}_d^j\right)\right| \exp\left[-\left(\vec{r}_a^i-\vec{r}_d^j\right)^2/4\sigma^2\right]/(4\pi\sigma^2)^{3/2}$$

(Equation 4)

In this expression, parameters of individual axonal and dendritic segments arise from the skeleton densities of arbors with soma positions $\vec{R}_a$ and $\vec{R}_d$ (Equation 1 of this box). The number of potential synapses calculated from Equation 4 strongly depends on the details of arbor geometries and neuron positions in the template, but typically stays >1 in the cortical column [7,23,24,27,33].

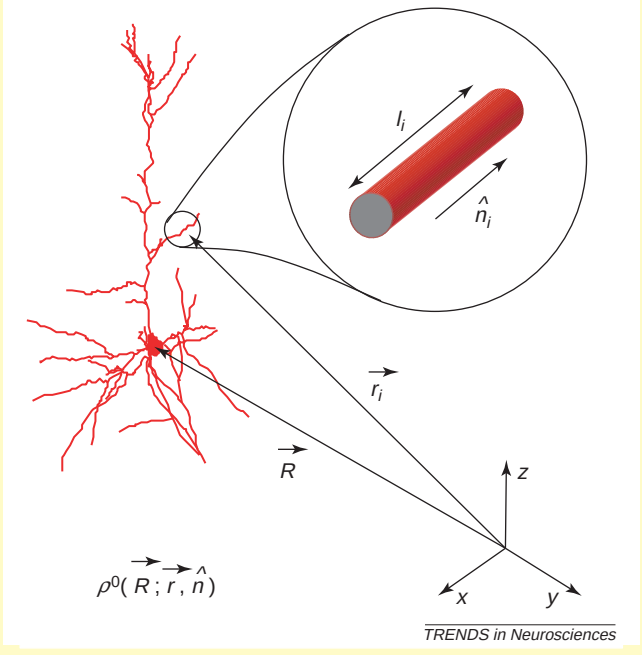

Figure I. Skeleton density. The dendritic arbor from Figure 1(a) of the main text is reconstructed as a set of straight connected segments of lengths l_i and orientations $\hat{n}_i$ (inset). Vector $\vec{R}$ indicates soma position in the template, and $\vec{r}_i$ specifies the position of i-th segment center. Skeleton density of the arbor is denoted by ρ^0.

positions. Similar maps have been reported in rodent cortex [7,27].

Although potential connectivity exhibits layer specificity, the expected number of potential synapses among excitatory spiny neurons is greater or equal to one over a few-hundred microns (white contours in Figure 2). This length scale is often associated with the cortical column [28] (intermediate between the minicolumn [29–31] and the hypercolumn [32]). Therefore, potential connectivity maps could provide a geometric definition for a cortical column as a domain where potential synapses exist between most neurons or, in other words, where potential connectivity is all-to-all [23,24,27,33].

Comparison of potential and functional synaptic connectivity

What can potential connectivity tell us about circuit function in terms of the neuronal activity? Because neuronal dynamics is determined by electrical inputs from (non-silent) actual or functional synapses, their relationship to potential synapses must be determined. One immediate observation is that the absence of

potential synapses between two neurons implies the absence of a functional connection between them. And, in general, the average number of actual synapses can be obtained from the number of potential synapses by multiplying it with the filling fraction [16]. The filling fraction is defined as the average ratio of actual to potential synapses for a given projection; estimates of the filling fraction for various cortical structures yield values of 0.1–0.3 [16].

We note that proportionality between the numbers of actual and potential synapses does not hold for individual neuron pairs. Although nearby neurons are expected to have a few potential synapses, the number of actual synapses is distributed bi-modally, with a large fraction of pairs being unconnected (e.g. see [27,34,35]), and the strength of synaptic connections in local circuits is highly variable [36,37]. Instead, the strength of a connection between a pair of local neurons is correlated with the number of touches between dendritic spines and axonal boutons that can be identified using light microscopy [27].

But the average number of actual synapses and the strength of a projection between groups of neurons (e.g. between cortical layers) can be given by multiplying the filling fraction by the number of potential synapses. This is a variation of the hypothesis known as Peters' rule [4,6,9,38,39], which postulates that, on average, input to a postsynaptic neuron is proportional to the densities of presynaptic boutons. The relationship between potential and functional connectivity has been tested experimentally for several intracortical projections in the rat barrel cortex [40]. Functional connectivity has been measured using laser-scanning photostimulation [41,42] and compared with geometric connectivity derived from reconstructions of axons of presynaptic neurons and dendrites of postsynaptic neurons. The extent to which potential connectivity predicts functional connectivity varies from projection to projection (Figure 3). Although geometric connectivity is often well correlated with function, there are important differences indicating that there is additional specificity, not captured by such geometric analysis. Next, we explore how such specificity could have arisen.

Correlation between axons and dendrites: indication of geometric specificity

Calculation of the expected potential synapse number (Box 1) is based on the assumption that the spatial positions of axonal and dendritic branches are uncorrelated. But is such assumption justified? To answer this question, counted numbers of potential synapses between pairs of neurons, reconstructed jointly in 3D, were compared with numbers expected for uncorrelated arbors [43] (Box 2). For cortical neurons, the answer depends on the neuron class and connectedness. Pyramidal neuron axons are uncorrelated with their postsynaptic targets (see also [27]), which is consistent with the observation that pyramidal axons are relatively straight [44] (Figure 4a). By contrast, GABAergic neuron axons are correlated with their postsynaptic targets, consistent with the higher tortuosity and branching in these axons (Figure 4b). The functional importance of this finding is

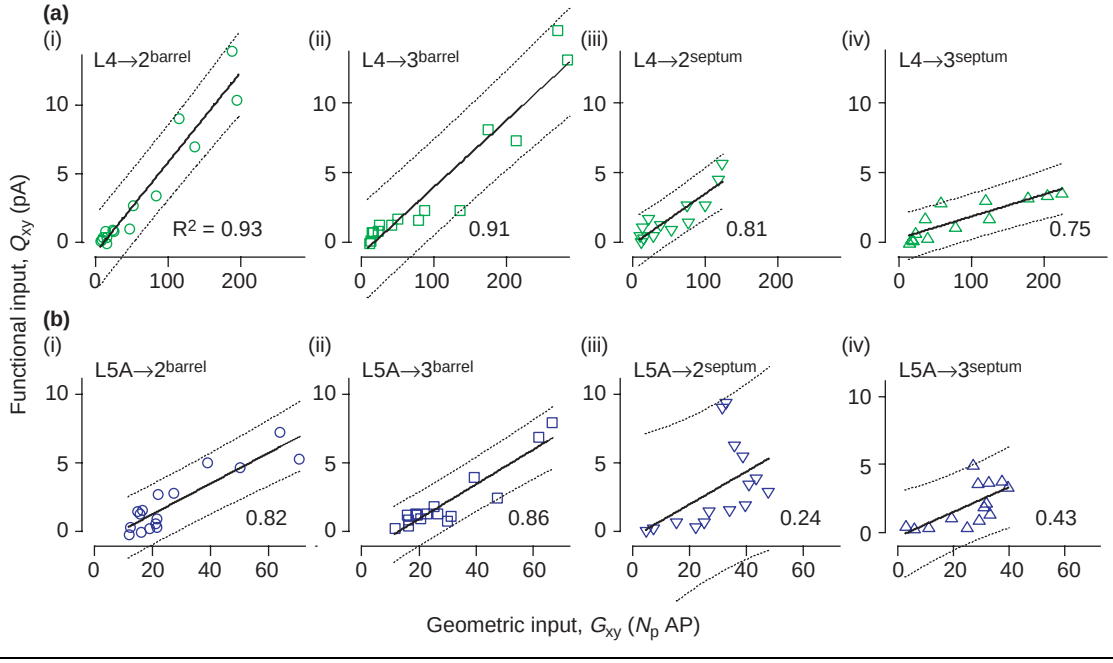

Figure 3. Comparison of measured functional inputs (Q_{xy}) with predicted geometric inputs (G_{xy}) for eight different intracortical projections in the rat barrel cortex. Q_{xy} is a current in a postsynaptic neuron in response to laser scanning photostimulation of clusters of presynaptic neurons at different lateral locations (individual points). G_{xy} is the number of action potentials predicted (from neurogeometry) to impinge onto all potential synapses of the postsynaptic neuron in response to photostimulation. **(a)** Average currents and numbers of action potentials in response to stimulation in layer 4, recorded in layer 2 (i) and layer 3 (ii) neurons in the barrel-related column, and in layer 2 (iii) and layer 3 (iv) neurons in the septum-related column. **(b)** Average currents and numbers of action potentials in response to stimulation in layer 5A, recorded in layer 2 (i) and layer 3 (ii) neurons in the barrel-related column, and in layer 2 (iii) and layer 3 (iv) neurons in the septum-related column. R^2 values for straight-line fits are shown. The dotted lines show 95% double-sided confidence intervals to the fits. Note different *x*-axis scale for layer-5A-originating projections. Modified, with permission, from [40].

emphasized by the fact that no correlations were detected within unconnected neuron pairs. In addition to detecting correlations, the ratio between the number of potential synapses observed experimentally and that expected for uncorrelated arbors was determined. As anticipated, this ratio for pyramidal axons is not significantly different from one. For axons of GABAergic neurons, the average ratios between the observed and expected numbers of potential synapses in connected pairs range between 1.3 and 2.7. These ratios can be used to correct the estimates of potential synapse numbers (Box 1) obtained using arbor densities.

Correlation between axonal and dendritic arbors is an indication of geometric specificity – that is, specificity in the spatial layout of axons and dendrites. Although there have long been examples of geometric specificity manifested in targeting of somata and axon initial segments [45–49], existence of geometric specificity for neocortical axon–dendrite synapses (Figure 4) was demonstrated for the first time in Ref. [43]. This specificity can be the result of several developmental mechanisms, such as growth cone guidance [50], pulling or guiding of existing axonal segments by dendritic filopodia [51], and specific branching or pruning [52–54].

Potential-to-actual synapse conversion can implement synaptic specificity

As reviewed here, axons of cortical pyramidal neurons are not correlated with their targets, implying no geometric specificity. Does this mean that synaptic connections between pyramidal neurons are not specific [6]? Not necessarily. Specificity can be implemented on the level of individual synapses by selectively converting potential synapses into actual ones (Figure 4a, bottom). It is convenient for further discussion to switch from the axon-centric view of Figure 4 to the dendrite-centric point of view of Figure 5. This figure illustrates that selectively choosing which presynaptic axons synapse on a given dendrite is possible only if the filling fraction [16] is less than one. Then, determining whether there is room for structural synaptic specificity requires evaluating the filling fraction in the neuropil.

Estimating the filling fraction directly using light microscopy is currently impossible because every axon

Box 2. How to detect short-range correlations between axonal and dendritic arbors by counting potential synapses: the shift method

Correlations in spatial locations of axons and dendrites can be detected by comparing the observed number of potential synapses in joint 3D reconstructions of neuron pairs with that expected under the assumption of independence between axons and dendrites – that is, the control distribution of potential synapse counts. This distribution could be deduced by generalizing the approach described in Box 1, and applying it to the reconstructed arbor pairs. However, this method of generating the control distribution is not sufficiently sensitive because it ignores the details of branching structures of individual neurons. The shift method, which generates the distribution of potential synapse count, can overcome this difficulty [43]. This method destroys short-range correlation (if any) in branch positions between arbors, but preserves branching structures of individual arbors. *In silico*, one whole arbor is shifted relative to the other along a vector randomly chosen from a cube centered at the origin (Figure Ia,b of this box). By counting potential synapses after each shift, the control distribution is generated (Figure Ic). The size of the cube, typically 20–40 μm on the side, is chosen so that the shift is large enough to establish a different population of potential synapses (much larger than the spatial scale, s), and small enough to avoid altering arbor overlap significantly (much smaller than the arbor overlap scale of 100–200 μm). The results are typically not sensitive to small variations in the cube size.

Next, the arbor correlation coefficient C is introduced; it is confined to the $[-1,1]$ range. The absolute value of the correlation coefficient $|C|$ can be calculated as twice the area under the control distribution between the mean and the observed numbers of potential synapses (shaded area in Figure Ic of this box). C is positive if the observed numbers of potential synapses is greater than the mean of the control distribution, indicating attraction between arbors, and otherwise negative, indicating repulsion. Correlations can be detected at various scales by changing the value of s (Figure Id of this box).

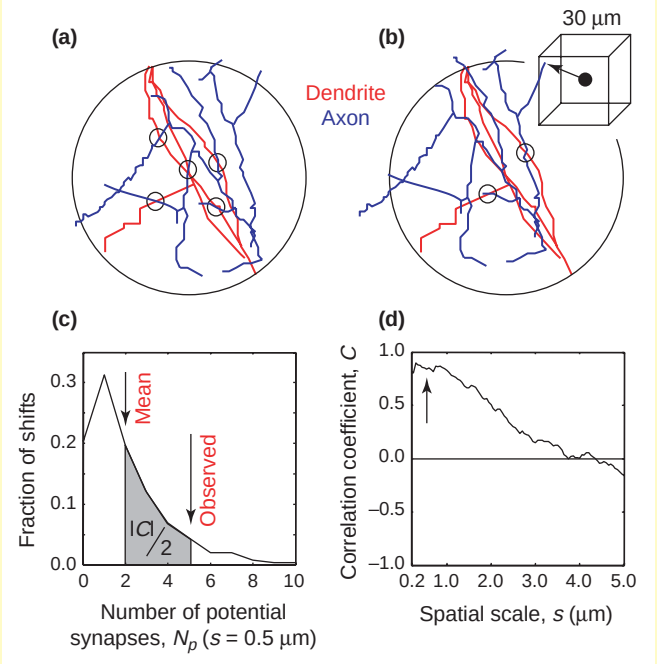

Figure I. Arbor correlation coefficient and the shift method. **(a)** Fragment of a 3D reconstruction of a pyramidal dendrite (red) and a regular spiking non-pyramidal cell axon (blue) from Figure 1(b) of the main text. Five potential synapses between the arbors (s=0.5 μm) are shown with small black circles. **(b)** After a small random shift of the axon (blue), the number of new potential synapses is smaller. The arrow shows the direction of the shift, randomly chosen from the 30 μm cube. **(c)** Control distribution of number of potential synapses for the same arbor pair. The observed numbers of potential synapses are larger than the mean of the control distribution. The absolute value of the arbor correlation coefficient $|C|$ is defined as twice the shaded area. **(d)** Arbor correlation coefficient (C) as function of spatial scale (s) for the same arbor pair. Correlation scale s=0.5 μm (arrowed) corresponds to distribution in (c). Modified, with permission, from [43].

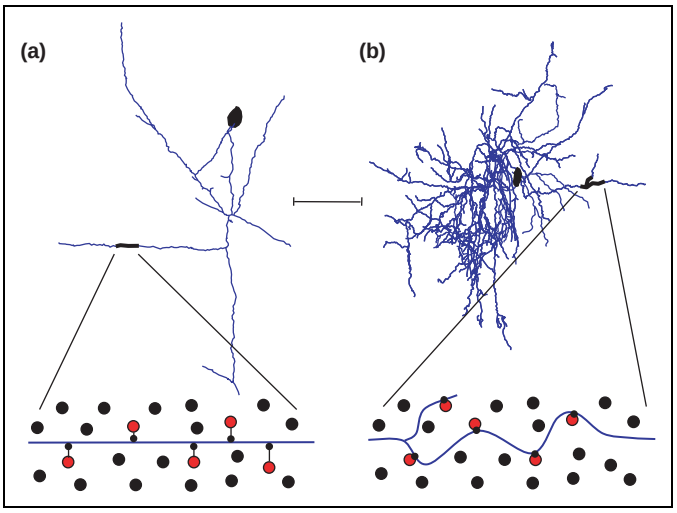

Figure 4. Examples of geometrically specific and non-specific layouts. **(a)** Pyramidal axon exhibits a non-specific layout with low tortuosity and relatively long branches (top). A magnification of the highlighted axonal segment (bottom) schematically shows locations of dendrites belonging to its postsynaptic (red circles) and all other (black circles) neurons. The axon shows no preference in its layout for one class of target over the other. Specificity can be implemented by establishing synapses on spines of some neurons but not others. **(b)** High tortuosity and branching of GABAergic axons could be a sign of specific layout. In a schematic magnification (bottom), the axonal segment of a neurogliaform cell shows layout that is specific with respect to its postsynaptic targets (red circles). Neurogliaform cell axons make most synapses onto dendritic shafts and spine necks. Scale bar, 100 μm. Modified, with permission, from [43].

and dendrite cannot be imaged simultaneously. Such estimates can be made by reconstructing neuropil volume around a dendritic branch [55] with serial-section electron microscopy and counting the numbers of potential and actual synapses. An indirect method, which combines light microscopy data with geometric analysis, can be less laborious [16] (Box 3). Such calculation of the filling fraction among cortical pyramidal neurons shows that the number of potential synapses exceeds the number of actual synapses by a factor of 3–9. This means that specificity can be implemented by selectively converting some potential synapses into actual ones.

Potential connectivity sets limits for structural synaptic plasticity

Small filling fractions for synapses among cortical pyramidal neurons suggests a structural plasticity mechanism, where synapses are re-arranged by eliminating existing spines and forming new ones (Figure 5). Such a mechanism has huge information-storage capacity and could be as important for learning and memory as changes of synaptic weights [16,33]. Experiments confirm that such re-arrangement takes place in developing and adult animals [56–58] and depends on neuronal activity patterns [59]. Limits for synaptic plasticity due to formation and elimination of spines are given by the estimates of potential connectivity. Then, the finding of all-to-all potential connectivity in the cortical column [23,24,27,33] paints a novel view of the local cortical circuit [27,33]. It suggests that a synaptic connection between any two excitatory spiny neurons within the cortical column can be implemented simply by spine growth. In other words, the local cortical circuit is imbedded in the potential connectivity domain. Therefore, the number of achievable circuits among excitatory spiny neurons in the cortical column is limited only by the space available to form new synapses [60].

Incidentally, observation of spine plasticity together with relative stability of dendrites and axons [57] suggests that the invariant description of synaptic connectivity should be based on the concept of potential connectivity. Then, the presence of a synapse should be characterized by a probability, meaning that the description of actual connectivity must be formulated statistically. This

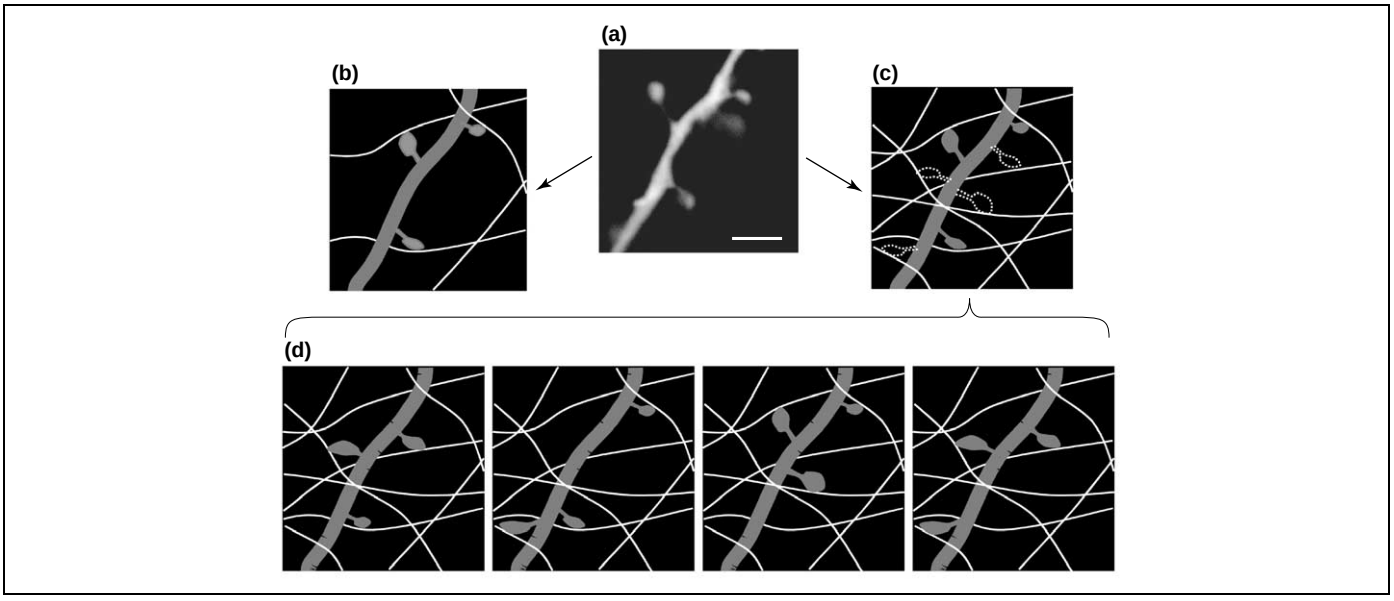

Figure 5. Structural synaptic specificity and plasticity in connectivity patterns. **(a)** Light microscopy image of a spiny dendritic branch. Scale bar, 2 μm. **(b)** Schematic drawing showing the dendrite in (a) together with nearby axons in one possible scenario. In this example, there is little or no potential for structural synaptic specificity or circuit reorganization because all axons within the spine length of a dendrite are already contacted. **(c)** The same dendrite in another scenario, where spine remodeling can contribute to circuit reorganization. Dendritic spines (solid gray) form actual synapses. Potential synapses include both actual synapses and other possible spine locations (dashed contours). **(d)** Some other synaptic connectivity patterns attainable from (c) by spine remodeling. The mammalian cortex looks more like scenario (c) than scenario (b), with large potential for structural synaptic specificity and plasticity. Adapted, with permission, from [16].

Box 3. How to estimate the filling fraction

The ratio of actual to potential synapses, called the filling fraction, can be calculated as follows. First, for a typical dendrite of a pyramidal neuron, the number of potential synapses is estimated. In other words, this is the number of axons passing through the cylinder of radius s surrounding the dendrite, where s is equal to the average spine length (Figure I of this box). Under several reasonable assumptions [16], this number can be expressed in terms of s, dendritic length per neuron L_d, and the linear density of axons (i.e. the total axon length per unit volume of neuropil) ρ_a:

$$N_p = \frac{\pi}{2} s L_d \rho_a. \quad \text{(Equation 1)}$$

Spine length and L_d can be measured using light microscopy, and ρ_a can be expressed in terms of the average inter-bouton interval b and the bouton density n_b. In turn, the bouton density is expressed (neglecting multiple-synapse boutons and the fraction of synapses onto inhibitory neurons) as the product of the neuron density (n) and average number of synapses per excitatory neuron (N) [16]:

$$\rho_a = b n_b \approx b n N. \quad \text{(Equation 2)}$$

From Equations 1 and 2 of this box, the ratio of actual to potential synapses (f) can be obtained using only parameters measurable by light microscopy:

$$f = \frac{N}{N_p} = \frac{2}{\pi s L_d b n}. \quad \text{(Equation 3)}$$

This calculation does not require the detailed knowledge of the axonal and dendritic arbor shapes. Equation 3 can be easily generalized to include multiple neuron classes and synapse types [16].

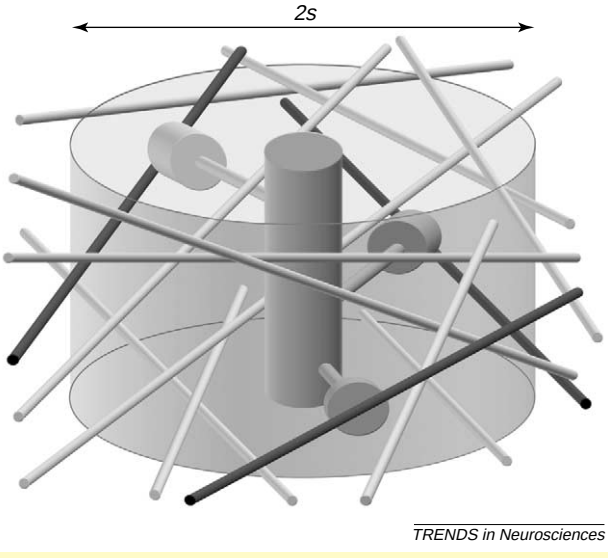

Figure I. Potential synapses. A fragment of a dendritic branch with three spines is surrounded by a cylinder of radius $s \sim 2$ μm (average spine length). Axons, which intersect the cylinder, establish potential synapses with the dendrite. Some of these axons make actual synaptic contacts with the dendritic spines (these axons are in black). For cortical pyramidal dendrites there are typically five times as many potential synapses as dendritic spines. To avoid clutter, axons are shown here as significantly thinner than typical cortical axons.

justifies use of the statistical approach outlined here for describing potential connectivity.

In conclusion, describing potential connectivity using neurogeometry takes us a step closer towards unraveling synaptic connectivity.

Acknowledgements

We thank Gordon Shepherd, Jr for numerous discussions and encouragement. We are grateful to Judith Hirsch, Luis Martinez, Zoltan Kisvarday and Alex Ferecskó for sharing their data and numerous discussions. This research was supported by the David and Lucille Packard Foundation, NIH, and the Klingenstein Foundation.

References

1 Ramón y Cajal, S. (1891) *Sur la structure de l'écorce cérébrale de quelques mammifères*. *Cellule* 7, 125–176
2 Sholl, D.A. (1956) *The Organization of the Cerebral Cortex*, Wiley, Methuen
3 Szentágothai, J. (1975) The 'module-concept' in cerebral cortex architecture. *Brain Res.* 95, 475–496
4 White, E.L. and Keller, A. (1989) *Cortical Circuits: Synaptic Organization of the Cerebral Cortex – Structure, Function, and Theory*, Birkhäuser
5 Abeles, M. (1991) *Corticonics: Neural Circuits of the Cerebral Cortex*, Cambridge University Press
6 Braitenberg, V. and Schüz, A. (1998) *Cortex: Statistics and Geometry of Neuronal Connectivity*, Springer
7 Kalisman, N. *et al*. (2003) Deriving physical connectivity from neuronal morphology. *Biol. Cybern.* 88, 210–218
8 Lubke, J. *et al*. (2003) Morphometric analysis of the columnar innervation domain of neurons connecting layer 4 and layer 2/3 of juvenile rat barrel cortex. *Cereb. Cortex* 13, 1051–1063
9 Binzegger, T. *et al*. (2004) A quantitative map of the circuit of cat primary visual cortex. *J. Neurosci.* 24, 8441–8453
10 Gilbert, C.D. (1983) Microcircuitry of the visual cortex. *Annu. Rev. Neurosci.* 6, 217–247
11 Gilbert, C.D. and Wiesel, T.N. (1981) Laminar specialization and intracortical connections in cat primary visual cortex. In *The Organization of the Cerebral Cortex* (Schmitt, F.O. *et al*., eds), pp. 163–191, MIT Press
12 Ascoli, G.A. *et al*. (2001) Generation, description and storage of dendritic morphology data. *Philos. Trans. R. Soc. Lond. B Biol. Sci.* 356, 1131–1145
13 Scorcioni, R. *et al*. (2004) Quantitative morphometry of hippocampal pyramidal cells: differences between anatomical classes and reconstructing laboratories. *J. Comp. Neurol.* 473, 177–193
14 Jefferis G.S.X.E. *et al*. (2005) Mapping higher olfactory centers in *Drosophila*. In *2005 Abstract book, Imaging neurons & neural activity: New methods, new results*. Program number 3. Cold Spring Harbor Laboratory Press
15 Jacobs, G.A. and Pittendrigh, C.S. (2002) Predicting emergent properties of neuronal ensembles using a database of individual neurons. In *Computational Neuroanatomy: Principles and Methods* (Ascoli, G.A., ed.), pp. 151–170, Humana Press
16 Stepanyants, A. *et al*. (2002) Geometry and structural plasticity of synaptic connectivity. *Neuron* 34, 275–288
17 Peters, A. and Kaiserman-Abramof, I.R. (1970) The small pyramidal neuron of the rat cerebral cortex. The perikaryon, dendrites and spines. *Am. J. Anat.* 127, 321–355
18 Spacek, J. and Hartmann, M. (1983) Three-dimensional analysis of dendritic spines. I. Quantitative observations related to dendritic spine and synaptic morphology in cerebral and cerebellar cortices. *Anat. Embryol. (Berl.)* 167, 289–310
19 Harris, K.M. (1999) Structure, development, and plasticity of dendritic spines. *Curr. Opin. Neurobiol.* 9, 343–348
20 Peters, A. *et al*. (1991) *The Fine Structure of the Nervous System: Neurons and their Supporting Cells*, Oxford University Press
21 White, J. *et al*. (1986) The structure of the nervous system of the nematode *Caenorhabditis elegans*. *Philos. Trans. R. Soc. Lond. B Biol. Sci.* 314, 1–340
22 Durbin, R. (1987) *Studies on the Development and Organisation of the Nervous System of* Caenorhabditis elegans, Cambridge University Press
23 Stepanyants, A. *et al.* (2003) Domains of potential connectivity of cortical spiny neurons. Program number 911.18. In *2004 Abstract Viewer and Itinerary Planner*, Society for Neuroscience, online (http://sfn.scholarone.com/itin2003/)
24 Stepanyants, A. *et al.* (2004) Potential connectivity in local cortical circuits. Program number 359 (T40). In *2004 Abstract Book*, Organization for Computational Neurosciences, online (http://www.cnsorg.org/Abstract_Book.pdf)

25 Hirsch, J.A. *et al*. (1998) Ascending projections of simple and complex cells in layer 6 of the cat striate cortex. *J. Neurosci.* 18, 8086–8094
26 Kisvarday, Z.F. *et al*. (2002) One axon-multiple functions: specificity of lateral inhibitory connections by large basket cells. *J. Neurocytol.* 31, 255–264
27 Kalisman, N. *et al*. (2005) The neocortical microcircuit as a tabula rasa. *Proc. Natl. Acad. Sci. U. S. A.* 102, 880–885
28 Hubel, D.H. and Wiesel, T.N. (1963) Shape and arrangement of columns in cat's striate cortex. *J. Physiol.* 165, 559–568
29 Peters, A. and Payne, B.R. (1993) Numerical relationships between geniculocortical afferents and pyramidal cell modules in cat primary visual cortex. *Cereb. Cortex* 3, 69–78
30 Mountcastle, V.B. (1997) The columnar organization of the neocortex. *Brain* 120, 701–722
31 Rockland, K.S. and Ichinohe, N. (2004) Some thoughts on cortical minicolumns. *Exp. Brain Res.* 158, 265–277
32 Hubel, D.H. and Wiesel, T.N. (1977) Ferrier lecture. Functional architecture of macaque monkey visual cortex. *Proc. R. Soc. Lond. B. Biol. Sci.* 198, 1–59
33 Chklovskii, D.B. *et al*. (2004) Cortical rewiring and information storage. *Nature* 431, 782–788
34 Markram, H. *et al*. (1997) Physiology and anatomy of synaptic connections between thick tufted pyramidal neurones in the developing rat neocortex. *J. Physiol.* 500, 409–440
35 Feldmeyer, D. *et al*. (2002) Synaptic connections between layer 4 spiny neurone–layer 2/3 pyramidal cell pairs in juvenile rat barrel cortex: physiology and anatomy of interlaminar signalling within a cortical column. *J. Physiol.* 538, 803–822
36 Ikegaya, Y. *et al*. (2004) Synfire chains and cortical songs: temporal modules of cortical activity. *Science* 304, 559–564
37 Song, S. *et al*. (2005) Highly nonrandom features of synaptic connectivity in local cortical circuits. *PLoS Biol.* 3, e68
38 Peters, A. and Feldman, M.L. (1976) The projection of the lateral geniculate nucleus to area 17 of the rat cerebral cortex. I. General description. *J. Neurocytol.* 5, 63–84
39 Peters, A. (1979) Thalamic input to the cerebral cortex. *Trends Neurosci.* 2, 183–185
40 Shepherd, G.M. *et al*. (2005) Geometric and functional organization of cortical circuits. *Nat. Neurosci*. doi: 10.1038/nn1447 (http://www.nature.com/neuro/index.html)
41 Callaway, E.M. and Katz, L.C. (1993) Photostimulation using caged glutamate reveals functional circuitry in living brain slices. *Proc. Natl. Acad. Sci. U. S. A.* 90, 7661–7665
42 Shepherd, G.M. *et al*. (2003) Circuit analysis of experience-dependent plasticity in the developing rat barrel cortex. *Neuron* 38, 277–289
43 Stepanyants, A. *et al*. (2004) Class-specific features of neuronal wiring. *Neuron* 43, 251–259
44 Thomson, A.M. and Morris, O.T. (2002) Selectivity in the interlaminar connections made by neocortical neurones. *J. Neurocytol.* 31, 239–246
45 Freund, T.F. (2003) *Interneuron Diversity series:* Rhythm and mood in perisomatic inhibition. *Trends Neurosci.* 26, 489–495
46 Freund, T.F. and Buzsaki, G. (1996) Interneurons of the hippocampus. *Hippocampus* 6, 347–470
47 Somogyi, P. (1977) A specific 'axo-axonal' interneuron in the visual cortex of the rat. *Brain Res.* 136, 345–350
48 Somogyi, P. *et al*. (1998) Salient features of synaptic organisation in the cerebral cortex. *Brain Res. Rev.* 26, 113–135
49 Wang, Y. *et al*. (2002) Anatomical, physiological, molecular and circuit properties of nest basket cells in the developing somatosensory cortex. *Cereb. Cortex* 12, 395–410
50 Tessier-Lavigne, M. and Goodman, C.S. (1996) The molecular biology of axon guidance. *Science* 274, 1123–1133
51 Fiala, J.C. *et al*. (1998) Synaptogenesis via dendritic filopodia in developing hippocampal area CA1. *J. Neurosci.* 18, 8900–8911
52 Cline, H.T. (2001) Dendritic arbor development and synaptogenesis. *Curr. Opin. Neurobiol.* 11, 118–126
53 Ruthazer, E.S. *et al*. (2003) Control of axon branch dynamics by correlated activity *in vivo*. *Science* 301, 66–70
54 Scott, E.K. and Luo, L. (2001) How do dendrites take their shape? *Nat. Neurosci.* 4, 359–365
55 Sorra, K.E. and Harris, K.M. (2000) Overview on the structure, composition, function, development, and plasticity of hippocampal dendritic spines. *Hippocampus* 10, 501–511
56 Lendvai, B. *et al*. (2000) Experience-dependent plasticity of dendritic spines in the developing rat barrel cortex *in vivo*. *Nature* 404, 876–881
57 Trachtenberg, J.T. *et al*. (2002) Long-term *in vivo* imaging of experience-dependent synaptic plasticity in adult cortex. *Nature* 420, 788–794
58 Holtmaat, A.J. *et al*. (2005) Transient and persistent dendritic spines in the neocortex *in vivo*. *Neuron* 45, 279–291
59 Nagerl, U.V. *et al*. (2004) Bidirectional activity-dependent morphological plasticity in hippocampal neurons. *Neuron* 44, 759–767
60 Chklovskii, D.B. *et al*. (2002) Wiring optimization in cortical circuits. *Neuron* 34, 341–347
61 Hellwig, B. (2000) A quantitative analysis of the local connectivity between pyramidal neurons in layers 2/3 of the rat visual cortex. *Biol. Cybern.* 82, 111–121
62 Anderson, J.C. *et al*. (1999) Dendritic asymmetry cannot account for directional responses of neurons in visual cortex. *Nat. Neurosci.* 2, 820–824
63 Yoshioka, T. *et al*. (1996) Relation between patterns of intrinsic lateral connectivity, ocular dominance, and cytochrome oxidase-reactive regions in macaque monkey striate cortex. *Cereb. Cortex* 6, 297–310
64 Liley, D.T.J. and Wright, J.J. (1994) Intracortical connectivity of pyramidal and stellate cells: estimates of synaptic densities and coupling symmetry. *Network Comp. Neural Syst.* 5, 175–189
65 Uttley, A.M. (1955) The probability of neural connexions. *Proc. R. Soc. Lond. B. Biol. Sci.* 144, 229–240
66 Uttley, A.M. (1956) *Cortical Circuits: Synaptic Organization of the Nervous System*, Birkhaüser